

Magnetic properties of biocompatible CoFe_2O_4 nanoparticles using a facile synthesis

Annrose Sunny^{a,b}, Aneesh Kumar K.S.^a, Varsha Karunakaran^{b,d}, Aathira M.^a,
Geeta R. Mutta^c, Kaustabh K. Maiti^d, V. Raghavendra Reddy^e, M. Vasundhara^{a,*}

^a Materials Science and Technology Division, CSIR-National Institute for Interdisciplinary Science and Technology, Industrial Estate, Trivandrum 695 019, India

^b Academy of Science and Innovative Research, CSIR, New Delhi, India

^c Nano-Materials Laboratory, School of Engineering and Physical Sciences, Heriot Watt University, Edinburgh EH144 AS, United Kingdom

^d Chemical Science and Technology Division, Organic Chemistry Section, CSIR-National Institute for Interdisciplinary Science and Technology, Industrial Estate, Trivandrum 695 019, India

^e UGC-DAE Consortium for Scientific Research, University Campus, Khandwa Road, Indore 452001, India

ARTICLE INFO

Article history:

Received 2 August 2017

Received in revised form 16 April 2018

Accepted 18 April 2018

ABSTRACT

Cobalt ferrite (CoFe_2O_4) nanoparticles were synthesised by a simple and cost-effective method using Co and Fe nitrates and freshly extracted egg white in an aqueous medium. X-ray diffraction patterns and Selected Area Electron Diffraction (SAED) pattern results indicate that the CoFe_2O_4 nanoparticles have spinel structure with $Fd\bar{3}m$ space group. The average particle size of CoFe_2O_4 nanoparticles is found to be from 45 nm. Temperature and field dependence of magnetisation reveals that the CoFe_2O_4 nanoparticles form ferrimagnetic in nature. A null cytotoxicity is observed in the CoFe_2O_4 nanoparticle which indicates that the material has an excellent biocompatibility. In order to check the importance of CoFe_2O_4 nanoparticles using the egg-white synthesis, the structural, magnetic and cytotoxicity of CoFe_2O_4 nanoparticles prepared via egg white method have been compared with that of sol-gel method. The egg-white method adopted in the present study appears to be a promising route of CoFe_2O_4 nanoparticles for biomedical applications.

© 2018 Elsevier B.V. All rights reserved.

1. Introduction

Spinel ferrite nanoparticles (NPs) with the general formula MFe_2O_4 ($M = \text{Cr, Mn, Co, Ni, Cu}$ and Zn) are one of the important class of materials because of their unique magnetic and electrical transport properties with a good chemical and thermal stabilities. Technologically, these materials are very promising and have been used in several applications, including magnetic recording, electronics, biomedicine, catalysis, sensors and pigments etc. [1–5]. Cobalt ferrite (CoFe_2O_4) NPs have good magnetostrictive, magneto crystalline anisotropy, high coercivity and moderate saturation magnetisation among all the ferrite family, which makes it competent to create a new turn in the existing world of ferrites. Moreover, they exhibit excellent chemical stability and mechanical hardness; a large magneto-optical effect; a high Curie temperature; and high electromagnetic performance [6,7]. In the past few years, CoFe_2O_4 NPs have reported to be used in several biomedical applications including therapeutic applications [8,9], remove malignant ovarian

cancer cells [10], and in controlled drug release [11]. Further, they have been tested in many of bio-assays like bacterial quantification study [12]. Therefore, CoFe_2O_4 NPs are potential candidates for several applications including biomedical applications.

There are several synthesis methods that have been explored for the preparation of CoFe_2O_4 NPs such as spray pyrolysis [13], auto combustion [14], sol-gel [15], citrate gel [16], chemical bath deposition [17], electrodeposition [18], spin coating [19], microemulsion [20], hydrothermal I [21], forced hydrolysis [22], reduction-oxidation route [23], and chemical synthesis [24] etc. However, these traditional methods have some drawbacks like agglomeration of prepared NPs and poor control in size and shape which greatly restrict them from the practical applications. Moreover, the traditional methods of synthesis of NPs require expensive and toxic reagents, complicated synthesis steps, high reaction temperatures and long reaction time. In the present study, CoFe_2O_4 NPs have been prepared using a simple and cost-effective method with Co and Fe nitrates and freshly extracted egg-white, hereafter named as Egg-white (EW) method and explored their structural, magnetic and cytotoxicity properties for the first time. The EW has the properties like gelling, foaming and emulsifying with high

* Corresponding author.

E-mail address: mvas@niist.res.in (M. Vasundhara).

nutrition qualities and also their solubility in water and its ability to unite with metal ions. This technique achieves less time for synthesising NPs with small particle size [25]. We synthesised CoFe₂O₄ NPs using the conventional sol–gel (SG) and EW method and made a comparison of structural, magnetic and cytotoxicity studies.

2. Experimental procedure

CoFe₂O₄ NPs were prepared in the present study using two methods. One is EW method and other one is conventional sol–gel method. In EW synthesis, high purity powders of cobalt nitrate (Co(NO₃)₂·6H₂O) (Alfa Aesar), Iron nitrate (Fe(NO₃)₂·9H₂O) (Alfa Aesar) and freshly extracted egg white were used as the starting materials. In a typical procedure, egg white was mixed with deionised water in 2:3 ratios and add stoichiometric amount of metals nitrate into it (For 3 g of sample preparation the amount of cobalt nitrate and Iron nitrate taken is (3.7353 g, 10.3343 g respectively) [26]. Then it undergoes vigorous stirring at room temperature until a homogeneous solution was obtained. The precursors were then added into this homogeneous solution and stirred the solution for 2 h. It was then heated using a hot plate at 80 °C with vigorous stirring for several hours until a dried precursor having dark brown colour was formed. The dried precursor was then crushed into powder using a mortar and pestle and calcined at 400 °C for 4 h followed by crushing and recalcination at 800 °C for 4 h. In SG synthesis, stoichiometric amount of high purity powders of cobalt nitrate (Co(NO₃)₂·6H₂O) (Alfa Aesar) and iron nitrate (Fe(NO₃)₂·9H₂O) (Alfa Aesar) were dissolved in a minimum amount of deionised water or ethylene glycol and stirred for half an hour. Then the solution was heated to 60 °C and citric acid was added followed by ethylene glycol. A particular molar ratio of citric acid to total moles of nitrate ions was maintained. The temperature of the solution was then increased gradually to 120 °C and kept constant for a long time to get the xerogel. It was then dried and a black precipitate was obtained. The dried precursor was then crushed into powder using a mortar and pestle and calcined at 400 °C for 4 h followed by crushing and recalcination at 800 °C for 4 h. The crystal structure and phase purity of the powdered compound were analysed using X-ray diffractometer (PANalytical-Empyrean) using Cu K_α radiation with wavelength 1.5404 Å and the scanning size of 0.01° from 20° ≤ θ ≤ 80°. Rietveld refinement of the diffraction patterns was carried out using Fullprof software. The particle morphology and sizes of samples prepared through EW and SG methods were directly investigated by high resolution transmission electron microscopy (HRTEM, JEOL-2010). The infrared spectra of the CoFe₂O₄ NPs were recorded using a Fourier transform infrared (FT-IR) spectrometer (Spectrum One FTIR Spectrometer, Perkin Elmer Instruments, USA) in the range 4000–370 cm⁻¹ with a resolution of 1 cm. Magnetic measurements of the samples were made as a function of temperature and applied field using a vibrating sample magnetometer attached to physical property measurement system (Quantum Design Inc., USA). Room temperature Mössbauer spectra have been recorded with in a velocity range ±15 mm/s in transmission geometry using a conventional constant accelerated spectrometer with a 57-Co(Rh) source and a standard PC-based Mössbauer spectrometer equipped with Wissel velocity drive. Velocity calibration of the spectrometer has been done with a natural Fe absorber at room temperature. Cell viability/cytotoxicity of CoFe₂O₄ NPs was studied using MTT assay (3-(4,5-dimethylthiazol-2-yl)-2,5-diphenyltetrazolium bromide) using HeLa cells [27]. HeLa cells were seeded at a density of 10⁴ cells/well in a 96 well plate and incubated at 37 °C for sufficient growth. The NPs of concentrations 50, 100, 250 and 500 μM were added to the wells separately. The treated cells were incubated for 24 h. The cells were then exposed to MTT at a concentration of

50 μg/well and again incubated for 3 h. The working solution of MTT was prepared in hanks balanced salt solution (HBSS). After viewing formazan crystals under the microscope, the crystals were solubilised by treating the cells with dimethyl sulfoxide (DMSO) isopropanol at a ratio of 1:1 for 20 min at 37 °C. Finally, the absorbance was measured by plate reader at 570 nm. The relative cell viability in percent was calculated as:

$$\text{Cell viability (\%)} = \frac{\text{Absorbance of treated}}{\text{Absorbance of control}} \times 100 \quad (1)$$

The cytotoxicity of the CoFe₂O₄ NPs was also determined by the lactate dehydrogenase (LDH) release assay on HeLa cells [28]. LDH release in the medium is due to the loss of membrane integrity either due to apoptosis or necrosis. HeLa cells were treated with different concentration (50, 100, 250 and 500 μM) of the compounds CoFe₂O₄ EW and CoFe₂O₄ SG for 24 h. Further 50 μl of the supernatant of the treated cell was transferred into new 96-well plates, and 50 μl of the LDH reaction solution (Pierce™ LDH Cytotoxicity Assay Kit, Thermo Scientific™, Pittsburgh, PA) was added for 30 min. Finally, the intensity of red colours in the sample indicating the LDH activity was measured at 490 nm using a Biotek Synergy 4 Multi-Mode Reader.

% Cytotoxicity

$$= \frac{\text{Compound treated LDH activity} - \text{Spontaneous LDH activity}}{\text{Maximum LDH activity} - \text{Spontaneous LDH activity}} \times 100 \quad (2)$$

where spontaneous LDH activity is the cells treated with sterile water and maximum LDH activity controls treated with 10X Lysis Buffer. The values are represented as the means ± SD of three separate experiments. In statistical analysis the data are expressed as the mean ± standard deviation (SD) of three replicates and analysed using Graph Pad PRISM software 5.0 (GraphPad Software Inc., San Diego, CA). One way analysis of variance (ANOVA) was used for the repeated measurements, and the differences were considered to be statistically significant if p < 0.05.

3. Results

Fig. 1 shows the powder XRD patterns of both the samples of CoFe₂O₄ NPs viz. SG (prepared through Sol Gel method) and EW (prepared through Egg White method). The peaks observed are typical of inverse spinel CoFe₂O₄ ferrite and the peak positions are in good agreement with the JCPDS file card number 89–0599. The ferrite phase was successfully refined to the cubic crystal structure with *Fd3m* space group. The lattice parameter obtained for EW NPs is 8.3869 Å and for SG NPs is 8.3843 Å respectively. In refinement, the oxygen positions (*x* = *y* = *z*) are taken as free parameters. However, all other atomic fractional positions are taken as fixed and other parameters such as occupancies; scale factors and shape parameter are chosen as free. The Rietveld refined parameters of both the samples are summarised in Table 1 which are in agreement with the previous reports [29].

Morphology of CoFe₂O₄ NPs synthesised by SG and EW NPs was investigated by transmission electron microscopy (TEM) as shown in Fig. 2. The NPs show somewhat polydisperse morphology with non-uniform sizes and the NPs also appear monodisperse with good crystalline structure which agree well with the XRD results. Selected area electron diffraction (SAED) patterns of the NPs are shown in Fig. 2(b,e) and the rings labelled in SAED pattern corresponds to the lattice planes and are identical to that of cubic spinel system [30]. To get the particle size distribution of NPs, we measured the size of 100 NPs selected from different images of the sample. The particle size distribution of the samples is obtained from their measured average diameters and is displayed in the histogram (Fig. 2 (c, f)). CoFe₂O₄ SG NPs has got an average particle

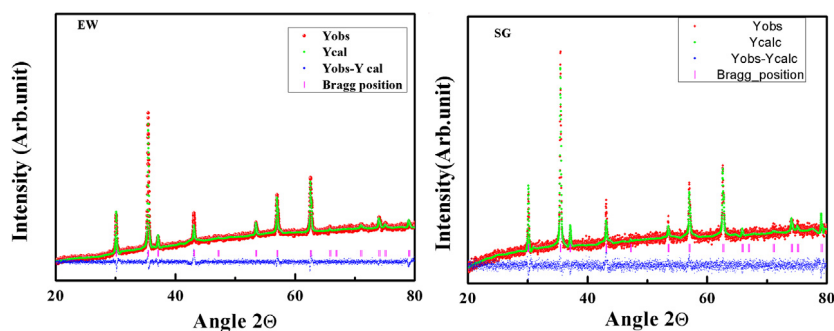


Fig. 1. Rietveld refinement patterns of CoFe_2O_4 EW and CoFe_2O_4 SG (Observation data are shown as (o) symbols, calculated and background intensities are shown as solid lines and the bottom line represents the difference between the measured and calculated intensities) NPs.

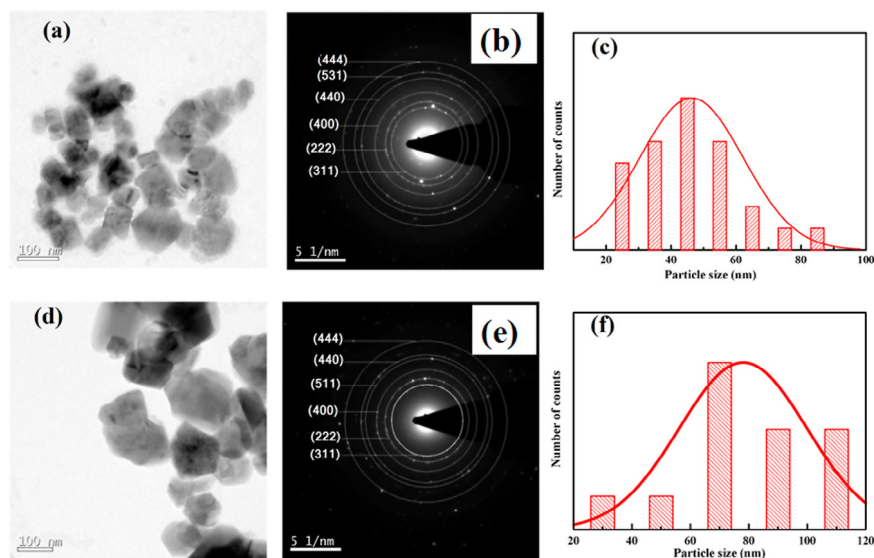


Fig. 2. TEM images, SAED pattern and particle size histograms of CoFe_2O_4 SG (a,b,c) and CoFe_2O_4 EW (d,e,f) NPs.

Table 1

Structural parameters obtained from the refinement output of CoFe_2O_4 SG and CoFe_2O_4 EW.

Sample (Fd3-m)	x	y	z	B_iso	Occ	²
EW						
O1	0.2473	0.2473	0.2473	-8.0729	1.3324	1.94
Fe2	0.50	0.50	0.50	-2.7387	0.7931	
Co2	0.50	0.50	0.50	-2.7387	0.3741	
Fe1	0.125	0.125	0.125	2.0894	0.6292	
Co1	0.125	0.125	0.125	2.0894	0.2764	
SG						
O1	0.2505	0.2505	0.2505	-9.02	0.33	1.29
Fe2	0.50	0.50	0.50	-2.51	0.42	
Co2	0.50	0.50	0.50	-2.51	0.25	
Fe1	0.125	0.125	0.125	8.46	0.99	
Co1	0.125	0.125	0.125	8.46	0.34	

size of around 80 nm (Fig. 2 c), whereas the average particle size of CoFe_2O_4 EW NPs is found to be 45 nm (Fig. 2(f)) in spite of the same preparation temperature is involved.

The information on the chemical changes taking place during the combustion process could be obtained by FTIR analysis. FTIR spectra of CoFe_2O_4 SG and CoFe_2O_4 EW NPs were carried out in the range 370–4000 cm^{-1} and depicted in Fig. 3. The high frequency absorption band observed in the range of 500 to 600 cm^{-1} indicates that the characteristic peak at 417 and 594 corresponds

to the motion of oxygen with respect to the tetrahedral and octahedral cations in the spinel ferrite NPs [31]. The EW sample had peaks at 1104–1630 cm^{-1} was due to the re-absorption of water molecules from the ambient atmosphere. The absorption band at 1630 cm^{-1} was due to the stretching frequency of the hydroxyl groups of absorbed water and the peak at 984 cm^{-1} representing the O-H outplane vibrations on the surface of EW sample which is absent in the case of SG sample. [32].

In order to understand the magnetic nature of the NPs synthesised using both the methods we have carried out the temperature and field variation of magnetic moment (M-T and M-H). Fig. 4 shows the temperature dependence of zero field cooled (ZFC) and field cooled (FC) magnetisation curves in the range of 2 K to 385 K of both the samples obtained under a constant magnetic field of 50 Oe. A clear bifurcation in FC and ZFC curves is observed in both the NPs, i.e., a rapid decrease in the ZFC curve with the decrease in temperature, whereas as FC curve response almost remains constant with the temperature. Precisely, in case of SG NPs, the FC magnetisation values gradually decreases with the decrease in temperature. But, in the case of EW NPs, the magnetisation values of FC curve gradually decreases with temperature up to 200 K and thereby remains a constant value down to 2 K. In general, FC and ZFC magnetisation curves are normally bifurcated due to the presence of super paramagnetic (SPM) relaxation of the nanoparticles, and this fact suggest that these samples may show SPM behaviour; however such behaviour is not seen in the present samples. It is also noteworthy that the FC magnetisation for EW

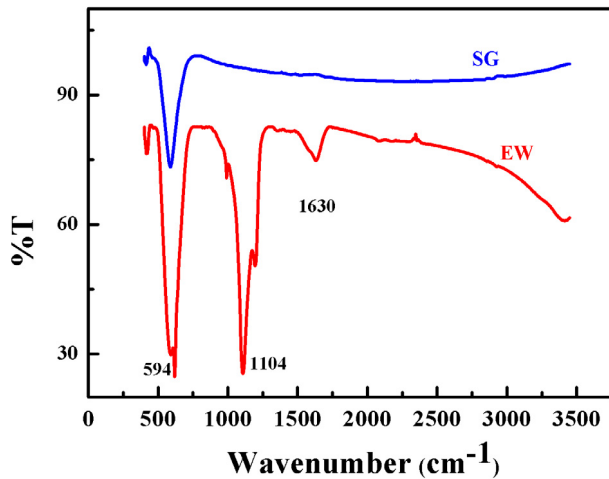


Fig. 3. FTIR spectra of CoFe₂O₄EW and CoFe₂O₄SG NPs.

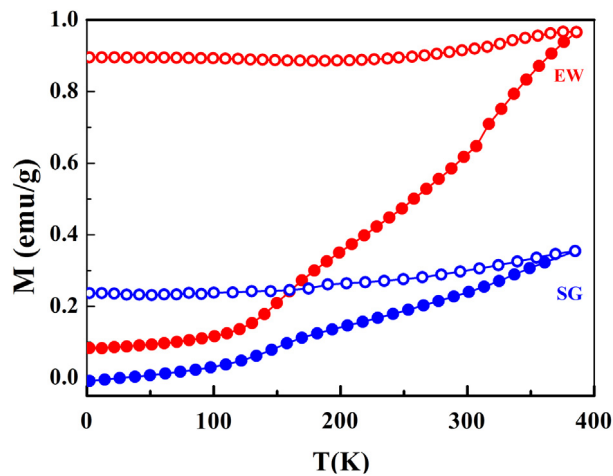


Fig. 4. Temperature dependent magnetisation curve of CoFe₂O₄ EW and CoFe₂O₄SG NPs. Open symbols represent the magnetisation taken under FC mode and Closed symbols represent ZFC mode.

is relatively high, which can be understood due to the increase in surface magnetisation with the decrease in particle size [33,34]. The field dependence of the magnetisation for both the samples measured at various temperatures in the range 300 to 2 K is shown in Fig. 5. The magnified image describing clear hysteric feature is also shown in the inset of each figure. From Fig. 5, it is clear that none of hysteresis curves support the SPM behaviour. Further,

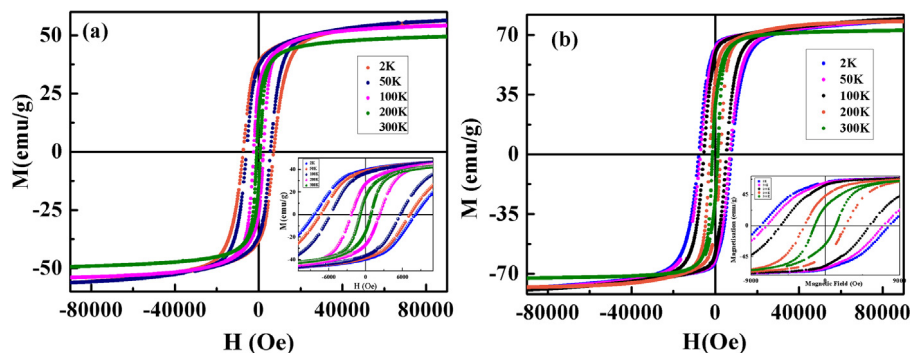


Fig. 5. Field dependence of magnetisation (MH) for (a) CoFe₂O₄ EW and (b) CoFe₂O₄ SG NPs.

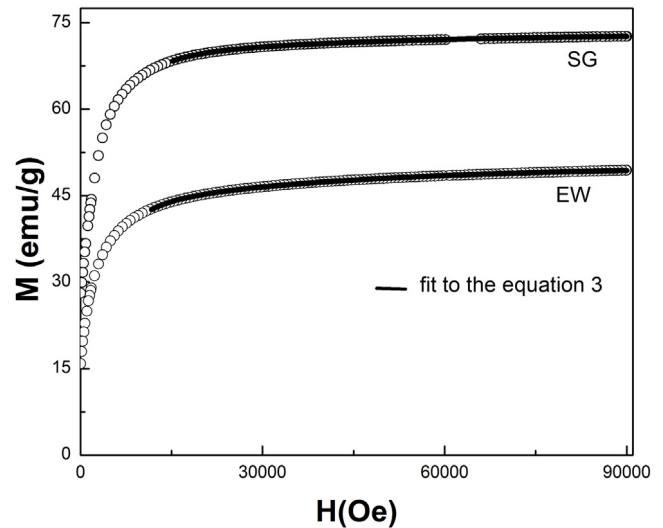


Fig. 6. Initial M-H curve at 300 K (black circle) along with the fits to Eq. (3) (Solid lines).

the M-H curves measured at all temperatures are found not to be perfectly saturated even at high fields for both samples. However, the non-saturating tendency is more prominently seen in the case of EW sample. This signifies little surface spin disorder in the EW samples. Further initial M-H curve measured at 300 K has been fitted to the below equation and shown in Fig. 6.

$$M(H) = M_{\text{sat}_f} \left(1 - \frac{b}{H^2} \right) + M_{\text{sat}_{sp}} \left(\coth \left(\frac{\mu H}{k_B T} \right) - \left(\frac{k_B T}{\mu H} \right) \right) \quad (3)$$

where M_{sat_f} represents ferrimagnetic state and $M_{\text{sat}_{sp}}$ represents SPM contribution. Here for EW sample- $M_{\text{sat}_f} = 44.09$ emu/g and $M_{\text{sat}_{sp}} = 7.14$ emu/g. For SG sample, $M_{\text{sat}_f} = 70.29$ emu/g and $M_{\text{sat}_{sp}} = 3.48$ emu/g. This quantifies, even though small SPM or surface spin contributes to ferrimagnetic saturation [35,36]. The coercivity (H_c), saturation magnetisation (M_s), remanant magnetisation (M_r), squareness ratio and particle size of both the samples are given in Table 2. The value of magnetisation obtained at the highest field of 90,000 Oe is taken as the saturation magnetisation. H_c , M_s and M_r of both the samples show moderately high values in compare to its bulk counterparts as mentioned in Table 2. The temperature variation of H_c for both the samples along with its bulk counterparts are plotted and shown in Fig. 7. The interesting feature from Fig. 7 is the exponential increase in the H_c with reduction in average crystallite size as mentioned in Table 2.

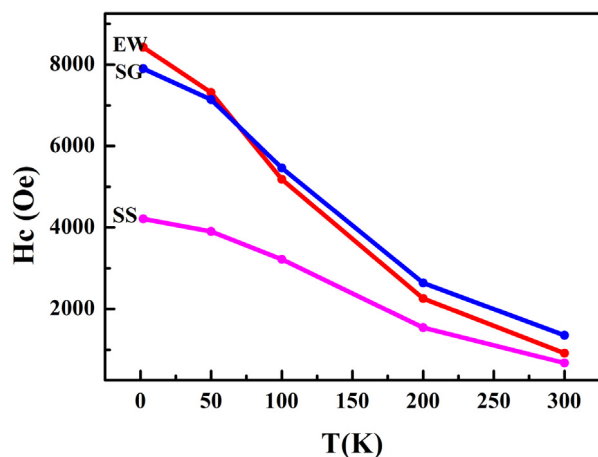
It can also be observed that the values of these parameters (H_c , M_s and M_r) decrease as the temperature increases from 2 K to

Table 2
Magnetic properties and the average particle size of the CoFe₂O₄ samples.

Sample	Average particle size (in nm)	Temperature (K)	H_c (Oe)	M_s (emu/g)	M_r (emu/g)	Squareness ratio (M_r/M_s)
SG	80	2	7901	79.7	66.9	0.84
		50	7141	72.7	64.7	0.89
		100	5461	71.5	60.6	0.85
		200	2640	70.2	51.1	0.73
		300	1291	69.4	44.7	0.64
EW	45	2	8426	56.6	40.9	0.72
		50	7314	55.2	40.2	0.72
		100	5181	54.4	37.9	0.70
		200	2255	53.1	31.6	0.60
		300	883	49.5	26.1	0.54
SS (Bulk compound synthesised by solid state method)	400 (the crystallite size is obtained from the SEM images)	2	4211	81.9	70.0	0.85
		50	3900	79.6	66.1	0.83
		100	3220	79.1	60.5	0.76
		200	1543	78.4	50.1	0.64
		300	672	74.8	42.7	0.57

Table 3
Hyperfine parameters obtained from room temperature Mössbauer spectra.

Sample name	Site	Line width (mm/s)	IS (mm/s)	2 (mm/s)	BHF (Tesla)	%Area	Area (mm/s)	χ^2
SG	A	0.39 ± 0.04	0.49 ± 0.01	0.022 ± 0.01	51.4 ± 0.08	26.98	0.058 ± 0.008	1.78
	B	0.43 ± 0.02	0.37 ± 0.01	0.013 ± 0.01	48.8 ± 0.03	73.02	0.156 ± 0.008	
	Total: 0.214 ± 0.011							
EW	A	0.26 ± 0.02	0.48 ± 0.006	−0.04 ± 0.01	51.5 ± 0.08	14.74	0.042 ± .0046	1.56
	B	0.47 ± 0.006	0.38 ± 0.002	0.003 ± 1e-4	48.7 ± 0.03	85.26	.245 ± 0.006	
	Total: 0.288 ± .007							

**Fig. 7.** Temperature variation of Coercivity for CoFe₂O₄ EW and CoFe₂O₄ SG NPs along with its bulk counterparts.

300 K. It is also remarkable that the value of saturation magnetisation decreases with the decrease in particle size (Table 2). The similar result is reported by Gabal et al. [26]. The magnetic performance of the ferrite structured nano materials is also influenced by the distribution of metal cations, which may be different from that of the bulk sample [34]. The most striking feature regarding the magnetic properties of the samples in the present study is the significant increase in the H_c value with the decrease of average particle size. The presence of large H_c may be attributed to the surface anisotropy, shape anisotropy, the chemical identity of Co due to the large orbital contribution to the magnetic moment and particle size, which is directly correlated to the H_c [34]. The squareness ratio of both the samples is found to be above 0.5, suggesting the particles are not in single domain [34]. Again, the magnetisation values observed are in good agreement with the

results reported in literature, e.g. 74.10 emu g^{−1} and 60.59 emu g^{−1} (net magnetisation value) [37]. The enhancement of magnetisation may be attributed to oxygen vacancies in the spinel. This can reduce the dead layer (spin disorder layer structure) as it has been previously described by Peddis et al. [37] and can result in values comparable or higher than its bulk counterparts. A similar behaviour has also been observed for NiFe₂O₄ [38] and ZnFe₂O₄ [39]. The magnetisation of EW NPs show more surface spin disorder in compare to SG NPs due to its smaller sizes.

Fig. 8(a, b) shows the room temperature Mössbauer spectra of the CoFe₂O₄ NPs synthesised through via SG and EW techniques. The Mössbauer spectra exhibited (sharp) six finger pattern of magnetic hyperfine field splitting for both the samples. The spectra have been fitted and analysed using NORMOS computer software (R.A. Brand, User Manual for NORMOS Software, 1992). Here we have used non linear least-squares minimisation technique with the Levenberg–Marquardt algorithm for deriving the spectral line parameters (Linewidth (Γ), Isomershift (IS), Quadrupole splitting (QS), Hyperfine field (Bhf), Area under the sextets (A)). The spectra have been fitted with two sextet components whose area are equivalent to Fe ions in two non-equivalent sites [tetrahedral Fe(A) and octahedral Fe(B)] of the spinel lattice structure. Refinement of the fitting of the experimental spectra has been repeated by allowing the variables like linewidth (Γ), Area under sextet(A), QS, Bhf, IS to vary while fixing the variables like relative line widths Γ_{23} (Γ_3/Γ_2) and relative area A13 (A3/A1), and A23 (A3/A1) of the absorption lines in each sextet. The quality of fitting has been checked by goodness of χ^2 value and matching of the refined pattern with observed spectra. The fitted parameters from room temperature Mössbauer spectra are given in Table 3. The sextet with hyperfine field 51.4T had an Isomer shift value 0.48 and the sextet with hyperfine field 48.8 had an Isomer shift value 0.38. These hyperfine fields and IS values are consistent to the values associated with Fe³⁺ ions at tetrahedral (A) and octahedral (B) sites, respectively, as reported for ferrite nanoparticles by various authors [40]. The low values of asymmetric shift, 2 and line width

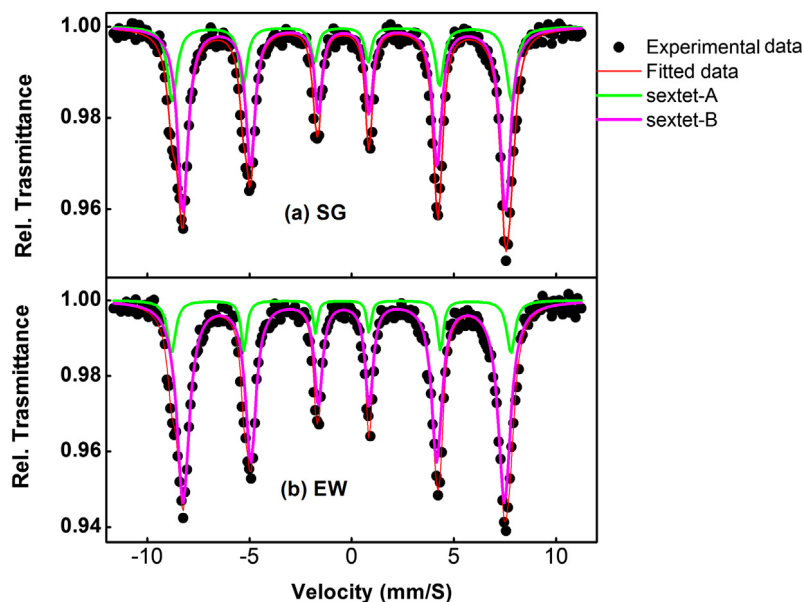


Fig. 8. Room temperature Mössbauer spectra of CoFe₂O₄ EW and CoFe₂O₄ SG NPs.

(<1 mm/s) points to the well ordered magnetic structure in the present samples [41].

In order to quantify the site occupancy of Fe ions at A and B sites of the spinel structure, the linear area ratio (or intensity ratio) associated with A and B sites (I_A/I_B) under the two sextets have been used. The general distribution of Co and Fe ions in CoFe₂O₄ NPs is: (Co_{1-x}²⁺Fe_x³⁺) [Co_x²⁺Fe_{2-x}³⁺] O₄ with $0 \leq x \leq 1$. The coordination factor x can be estimated by measuring the area ratio of tetrahedral (I_A) and octahedral (I_B) sextets from the Eq. (1)

$$\frac{I_A}{I_B} = \frac{f_A}{f_B} \times \frac{x}{(2-x)} \quad (4)$$

where f_A/f_B is the ratio of the recoilless fraction which is 0.94 at room temperature [42,43]. The estimated site distribution for SG sample is (Co_{0.44}²⁺Fe_{0.56}³⁺) [Co_{0.56}²⁺Fe_{1.44}³⁺] O₄. The distribution is close to the distribution (Co_{0.38}²⁺Fe_{0.62}³⁺) [Co_{0.62}²⁺Fe_{1.38}³⁺] O₄ reported by Murray and Linnet [44] for $x = 1.04$. For EW sample, the estimated distribution is (Co_{0.69}²⁺Fe_{0.31}³⁺) [Co_{0.31}²⁺Fe_{1.69}³⁺] O₄. These results are in good agreement with the earlier reports [45]. The magnetic moment calculated at room temperature in terms of Bohr magneton (μ_B) per formula unit (f.u) using the above estimated cation distribution for SG and EW samples are found to be $3.88 \mu_B/\text{f.u}$ and $4.38 \mu_B/\text{f.u}$ respectively. It is to be noted that the magnetic moment used for Co²⁺ and Fe³⁺ ions to be $3 \mu_B$ and $4 \mu_B$, respectively for calculating the moment from cation distribution (which is supposed to be maximum moment at 0 K). But, experimentally observed magnetic moment at room temperature using M-H curves for SG and EW samples are found to be $2.953 \mu_B/\text{f.u}$ and $1.85/\text{f.u}$ respectively, which are lesser values in that of the values, calculated using estimated cation distribution. This discrepancy is justified by taking into account of a considerable number of magnetic spins, either in surface or core of the particles, in disordered state at room temperature.

Bio-compatibility of the CoFe₂O₄ NPs is of major concern in biomedical applications. Therefore, in order to investigate the bio-compatibility of the NPs synthesised using both the methods, we assessed the cytotoxicity of the CoFe₂O₄ NPs. The effect of same on cell viability of HeLa cells in 24 h using MTT [46] assay and LDH [47] assay are shown in Fig. 8. Interestingly, it can be seen from Fig. 9(a) that the EW samples does not show any remarkable cytotoxicity even up to the concentration of 500 μM , but in the

case of SG sample the toxicity level increases with increasing the concentration level up to 500 μM . Fig. 9(b) shows a significant ($p < 0.001$) proliferation with EW NPs up to 250 μM and $p < 0.01$ for 500 μM . However, SG NPs shows some extent of toxicity at the concentrations of 250 μM ($p < 0.01$) and 500 μM ($p < 0.001$), but at lower doses it shows a tendency of non-toxic.

4. Discussion

CoFe₂O₄ NPs synthesised using both the methods are found to be crystallised into an inverse spinel structure, however, the particle size is found to be lesser in case of EW NPs even though the temperature involved is same for both the synthesis techniques. This could be due to the chelating nature of egg white involved in the synthesis techniques [48]. From the Mössbauer spectra it may be confirmed that SPM contribution is negligible. However, from the non saturated M-H curves, it is understood that the surface spins contribute to the magnetisation, resulting in such non-saturating tendency in the magnetisation even at such higher applied magnetic field, which is further verified by the slight broadening of absorption lines in Mössbauer spectra. The distribution of particles of different sizes of ferrimagnetic along with the contribution of surface spin lead to the overlapping of the tetrahedral and octahedral components in the absorption lines and subsequent broadened spectra [49,50]. It is observed that EW NPs have relatively more broadening in absorption lines when compared to SG NPs. This ascertains the fact that surface spin contribution is more in EW sample which is desirable for biomedical applications.

The biocompatibility of the CoFe₂O₄ NPs has been primarily analysed by two complementary assays viz., MTT and LDH, in which the former is a measure of cell viability and the latter shows the measure of cytotoxicity. Evaluating the extend of mitochondrial dehydrogenase activity in viable cells and cell membrane damage shown by the release of lactate dehydrogenase enzyme in non-viable cells indicated the non-toxic behaviour of EW NPs under all concentrations and SG NPs below 250 μM . Moreover, it can be seen from Fig. 8 that the viability of the cells is assessed by MTT assay which showed and cytotoxicity is evaluated by LDH assay which proved the safe nature of CoFe₂O₄ NPs prepared through EW method. Therefore, the bio-compatibility of CoFe₂O₄ NPs depends on the synthetic methods involved in which EW is confirmed to be more promising for the biomedical applications.

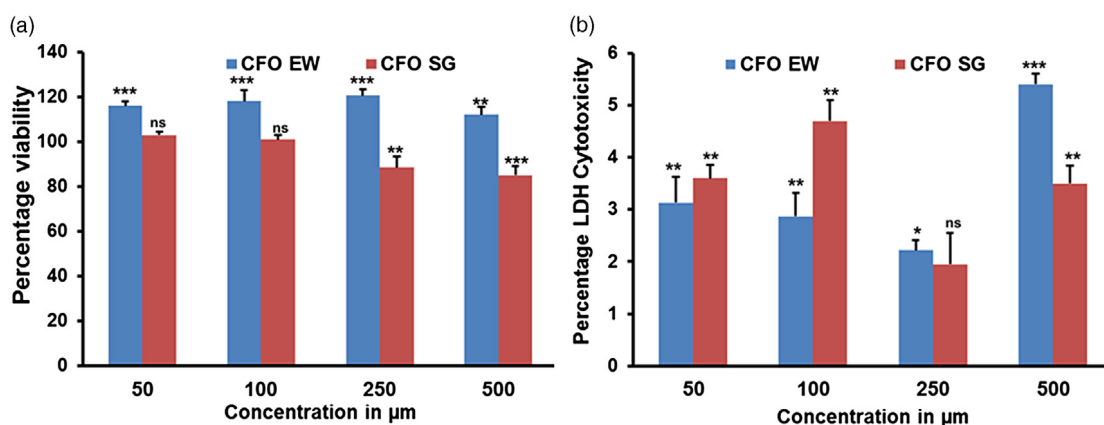


Fig. 9. Cell viability using (a) MTT and (b) LDH using HeLa cells after 24 h incubation with CoFe₂O₄ EW and CoFe₂O₄ SG samples in (a) MTT and (b) LDH assay. Datas are the mean \pm SD of three independent experiments; *** $p < 0.001$, ** $p < 0.01$, * $p < 0.05$; ns: not significant relative to control.

5. Conclusions

CoFe₂O₄ NPs have been synthesised by EW method and compared the results with that of made by CoFe₂O₄ NPs using SG synthesis. CoFe₂O₄ NPs formed in the lesser average particles of 45 nm in EW method. Magnetic properties decrease with the increase in temperature and suggest the ferrimagnetic nature down to 2 K. The existence of ferrimagnetic state is further explained by Mössbauer spectra, and confirmed that the estimated site distribution for SG sample is $(\text{Co}_{0.398}^{2+}\text{Fe}_{0.602}^{3+})[\text{Co}_{0.602}^{2+}\text{Fe}_{1.398}^{3+}]\text{O}_4$ and for EW sample, the estimated distribution is $(\text{Co}_{0.285}^{2+}\text{Fe}_{0.715}^{3+})[\text{Co}_{0.715}^{2+}\text{Fe}_{1.285}^{3+}]\text{O}_4$. The Cytotoxicity studies show that the NPs made by EW method are biocompatible up to 500 μM concentration. Overall it reveals that the CoFe₂O₄ NPs synthesised via EW method having superior properties like small particle size and less cytotoxic.

Acknowledgements

The authors would like to acknowledge the financial support received from Council of Scientific and Industrial Research (CSIR), Government of India, sponsored project no. CSC0132. Annrose Sunny is also thankful to Academy of Scientific and Innovative Research, CSIR. The authors would also like to thank Board of Research in Nuclear Sciences, sponsored project no. GAP 218939 for partially supporting this work.

References

- [1] G. Chandra, R.C. Srivastava, V.R. Reddy, H.M. Agarwall, Effect of sintering temperature on magnetization and Mössbauer parameters of cobalt ferrite nanoparticle, *J. Magn. Magn. Mater.* 427 (2017) 225–229.
- [2] P. Tartaj, M.M. Del Puerto, S.V. Veintemillas, T.C. Gonzales, C.J. Serna, The preparation of magnetic nanoparticles for applications in biomedicine, *J. Phys. D Appl. Phys.* 36 (2003) R 182–197.
- [3] C. Dey, K. Baishya, A. Ghosh, M.M. Goswami, A. Ghosh, K. Mandal, Improvement of drug delivery by hyperthermia treatment using magnetic cubic cobalt ferrite nanoparticles, *J. Magn. Magn. Mater.* 427 (2017) 168–174.
- [4] E. Tronc, P. Prene, J.P. Jolivet, J.L. Dormann, J.M. Greneche, Spin canting in Fe₂O₃, *Hyper Int.* 112 (1997) 97–100.
- [5] A.V. Raut, R.S. Barkule, D.R. Shengule, K.M. Jadhav, Synthesis structural investigation and magnetic properties of Zn²⁺ substituted cobalt ferrite nanoparticles prepared by the sol–gel auto-combustion technique, *J. Magn. Magn. Mater.* 358–359 (2014) 87–92.
- [6] C. Liu, A.J. Rondinone, Z.J. Zhang, Synthesis of magnetic spinel ferrite CoFe₂O₄ nanoparticles from ferric salt and characterization of the size-dependent superparamagnetic properties, *Pure Appl. Chem.* 72 (2000) 37–45.
- [7] J.P. Fortin, C. Wilhelm, J. Servais, C. Menager, J.C. Bacri, F. Gazeau, Size-sorted anionic iron oxide nanomagnets as colloidal mediators for magnetic hyperthermia, *J. Am. Chem. Soc.* 129 (2007) 2628–2635.
- [8] M.C. Franchini, G. Baldi, D. Bonacchi, D. Gentili, G. Giudetti, A. Lascialfari, M. Corti, P. Marmorato, J. Ponti, E. Micotti, U. Guerrini, L. Sironi, P. Gelosa, C. Ravagli, A. Ricci, Bovine serum albumin based magnetic nanocarrier for MRI diagnosis and hyperthermic therapy, a potential theranostic approach against cancer, *Small* 6 (2010) 366–370.
- [9] K.E. Scarberry, E.B. Dickerson, J.F. McDonald, Z.J. Zhang, Magnetic nanoparticle peptide conjugates for in vitro and in vivo targeting and extraction of cancer cells, *J. Am. Chem. Soc.* 130 (2008) 10258–10262.
- [10] V.V. Dhole, P.P. Khirade, C.M. Kale, V.G. Patil, N.D. Shinde, K.M. Jadhav, Crystallographic and infrared spectral investigations of Mg²⁺ substituted cobalt ferrite nanoparticles prepared by sol–gel auto combustion technique, *Int. J. Innov. Sci. Eng. Technol.* 2 (2015) 2348–7968.
- [11] D. Chaitali, B. Kaushik, G. Arup, M.G. Madhuri, G. Ajay, M. Kalyan, Improvement of drug delivery by hyperthermia treatment using magnetic cubic cobalt ferrite nanoparticles, *J. Magn. Magn. Mater.* 427 (2017) 168–174.
- [12] R.A. Hilgenbrink, P.S. Low, Folate receptor-mediated drug targeting from therapeutics to diagnostics, *J. Pharm. Sci.* 94 (2005) 2135–2146.
- [13] T.N. Patrusheva, S.A. Podorojnyak, K.P. Polyakova, S.D. Kirik, V.V. Menshikov, S.I. Levchenko, V.V. Patrushev, M.A. Adrianova, G.E. Gerasimova, Manufacturing solution for producing cobalt-ferrite films, *Chem. Mater. Eng.* 2 (2014) 33–36.
- [14] S. Kanagesan, M. Hashim, S. Tamilselvan, N.B. Alitheen, I. Ismail, M. Syazwan, M.M.M. Zuikimi, Sol–gel autocombustion synthesis of cobalt ferrite and its cytotoxicity properties, *Digest J. Nano Mater. Bio. Struct.* 8 (2013) 1601–1610.
- [15] R.A. Bortnic, F. Goga, A. Mesaros, M. Nasui, B. Stefan vasile, D. Roxana, L. Aavram, Synthesis of cobalt ferrite nanoparticles via a solgel a sol gel combustion method, *Studia UBB Chemia LXI 4* (2016) 213–222.
- [16] C. Cannas, A. Falqui, A. Musinu, D. Peddis, G. Piccaluga, CoFe₂O₄ nanocrystalline powders prepared by citrate–gel methods: Synthesis, structure and magnetic properties, *J. Nano Par. Res.* 8 (2006) 255–267.
- [17] V.S. Kumbhar, A.D. Jagadale, N.M. Shinde, C.D. Lokhande, Chemical synthesis of spinel cobalt ferrite (CoFe₂O₄) nano-flakes for supercapacitor application, *Appl. Surf. Sci.* 259 (2012) 39–43.
- [18] J.R. Scheffe, M.D. Allendorf, E.N. Coker, B.W. Jacobs, A.H. McDaniel, A.W. Weimer, Hydrogen production via chemical looping redox cycles using atomic layer deposition synthesized iron oxide and cobalt ferrites, *Chem. Mater.* 23 (2011) 2030–2038.
- [19] S.D. Sathaye, K.R. Patil, S.D. Kulkarni, P.P. Bakre, S.D. Pradhan, B.D. Sarwade, S.N. Shintre, Modification of spin coating method and its application to grow thin films of cobalt ferrite, *J. Mater. Sci.* 38 (2003) 29–33.
- [20] V. Pillai, D.O. Shah, Synthesis of high-coercivity cobalt ferrite particles using water-in-oil microemulsions, *J. Magn. Magn. Mater.* 163 (1996) 243–248.
- [21] L. Zhao, H. Zhang, Y. Xing, S. Shuyan, S. Yu, W. Shi, X. Guo, J. Yang, Y. Lei, F. Cao, Studies on the magnetism of cobalt ferrite nanocrystals synthesized by hydrothermal method, *J. Solid State Chem.* 181 (2008) 245–252.
- [22] N. Hanh, O.K. Quy, N.P. Thuy, L.D. Tung, L. Spinu, Synthesis of cobalt ferrite nanocrystallites by the forced hydrolysis method and investigation of their magnetic properties, *Physica B* 327 (2003) 382–384.
- [23] Z. Gu, X. Xiang, C. Fan, F. Li, Facile synthesis and characterization of cobalt ferrite nanocrystals via a simple reduction-oxidation route, *J. Phys. Chem. C* 112 (2008) 18459–18466.
- [24] K. Maaz, A. Mumtaz, S.K. Hasanain, A. Ceylan, Synthesis and magnetic properties of cobalt ferrite (CoFe₂O₄) nanoparticles prepared by wet chemical route, *J. Magn. Magn. Mater.* 308 (2007) 289–295.
- [25] Maensiri Santi, Masingboon Chivalart, A simple route to synthesize nickel ferrite (NiFe₂O₄) nanoparticles using egg white, *J. Script Mater.* 562 (2007) 797–800.

- [26] M.A. Gabal, A.A. Al-Juaid, S. El-Rashed, M.A. Hussein, Synthesis and characterization of nano-sized CoFe_2O_4 via facile methods: A comparative study, *Mater. Res. Bull.* 89 (2017) 68.
- [27] M. Gharibshahian, O. Mirzaee, M.S. Nourbakhsh, Evaluation of superparamagnetic and biocompatible properties of mesoporous silica coated cobalt ferrite nanoparticles synthesized via microwave modified pechini method, *J. Magn. Magn. Mater.* 425 (2017) 48–56.
- [28] A.A. Hisham, J.A. Mohd, A. Maqsood, Zinc ferrite nanoparticle-induced cytotoxicity and oxidative stress in different human cells, *Cell Biosci.* 5 (2015) 55.
- [29] M.A. Gabal, A.A. Al-Juaid, S. El-Rashed, M.A. Hussein, Synthesis and characterization of nano-sized CoFe_2O_4 via facile methods: A comparative study, *Mater. Res. Bull.* 89 (2017) 68.
- [30] L. Kumar, P. Kumar, A. Narayan, M. Kar, Rietveld analysis of xrd patterns of different sizes of nanocrystalline cobalt ferrite, *Int. Nano Lett.* 3 (2013) 8.
- [31] S. Mohapatra, R.R. Smruti, M. Swatilekha, K.M. Tapas, B.P. Asit, Monodisperse mesoporous cobalt ferrite nanoparticles synthesis and application in targeted delivery of antitumor drugs, *J. Mater. Chem.* 21 (2011) 9185–9193.
- [32] P. Thangaraj, J. Rajan, S. Durai, S. Kumar, A.R. Phani, G. Neri, The role of albumen (egg white) in controlled particle size and electrical conductivity behavior of zinc oxide nanoparticles, *Vacuum* 86 (2011) 140–143.
- [33] M. Vadivel, R. Ramesh Babu, K. Ramamurthi, M. Arivanandhan, Effect of pvp concentrations on the structural, morphological, dielectric and magnetic properties of CoFe_2O_4 magnetic nanoparticles, *Nano Struct. Nano Objects* 11 (2017) 112–123.
- [34] K.M.A. Zandi, H. Shokrollahi, L. Avazpour, M.R. Toroghinejad, Study on the effect of sol-gel parameters using the Taguchi technique to achieve the optimal crystallite size and magnetic properties of cobalt ferrite powders, *J. Sol-Gel Sci. Tech.* 76 (2015) 271–278.
- [35] S.J.S. Flora, V. Pachauri, Chelation in metal intoxication, *Int. J. Environ. Res. Publ. Health* 7 (2010) 2745–2788.
- [36] E.P. Wohlfarth, *HandBook of Magnetic Materials*, Vol. 3, North-Holland Publishing Company, 1982.
- [37] C. Vazquez-Vazquez, M.A. Lopez-Quintela, M.C. Bujan Nunez, J. Rivas, Finite size and surface effects on the magnetic properties of cobalt ferrite nanoparticles, *J. Nanopart. Res.* 13 (2011) 1663–1676.
- [38] D. Peddies, N. Yaacoub, M. Ferretti, A. Martinelli, G. piccaluga, A. Musinu, C. Cannas, G. Navarra, J.M. Greneche, D. Fiorani, Cationic distribution and sin canting in CoFe_2O_4 nanoparticles, *J. Phys.: Condens. Matter* 23 (2011) 426004.
- [39] P. Sivakumar, R. Ramesh, A. Ramanand, S. Ponnusamy, C. Muthamizhchelvan, Preparation and properties of nickel ferrite (NiFe_2O_4) nanoparticles via sol-gel auto-combustion method, *Mater. Res. Bul.* 46 (2011) 2204–2207.
- [40] D.S. Mathew, R.S. Juang, An overview of the structure and magnetism of spinel ferrite nanoparticles and their synthesis in microemulsions, *J. Chem. Eng.* 129 (2007) 51–65.
- [41] V. Sepelak, D. Baabe, F.J. Litterst, K.D. Becker, Structural disorder in the high-energy milled magnesium ferrite, *J. Appl. Phys.* 88 (2000) 5884–5894.
- [42] G.A. Sawatzky, F. Van Der Woude, A.H. Morrish, Recoilless-fraction ratios for Fe57 in octahedral and tetrahedral sites of a spinel and a garnet, *Phys. Rev.* 183 (1969) 383–386.
- [43] V. Sepelak, D. Baabe, D. Mienert, D. Schultze, F. Krumeich, F.J. Litterst, K.D. Becker, Evolution of structure and magnetic properties with annealing temperature in nanoscale high-energy-milled nickel ferrite, *J. Magn. Magn. Mater.* 257 (2003) 377–386.
- [44] J. Jacob, M.A. Khadar, Investigation of mixed spinel structure of nanostructured nickel ferrite, *J. Appl. Phys.* 107 (2010) 114310.
- [45] P.J. Murray, J.W.L. late, Cation distribution in the spinels $\text{Co}_x\text{Fe}_{3-x}\text{O}_4$, *J. Phys. Chem. Solids* 37 (1976) 1041–1042.
- [46] Michael V. Berridge, An S. Tan, Characterization of the cellular reduction of 3-(4,5-dimethylthiazol-2-yl)-2,5-diphenyltetrazolium bromide (MTT): Subcellular localization, substrate dependence, and involvement of Mitochondrial electron transport in MTT reduction, *Arch. Bio. Chem. Bio.* 303 (2) (1993) 474–482.
- [47] H. Xianglu, G. Robert, C. Nancy, W.M. Pamela, J. Jingkun, B. Pratim, N.F. Jacob, E. Alison, O. Gunter, Validation of an LDH assay for assessing nanoparticle toxicity, *Toxicology* 287 (2011) 99–104.
- [48] H.Le. Trong, L. Presmanes, E.D. Grave, A. Barnabe, C. Bonningue, P. Tailhades, Mössbauer characterisations and magnetic properties of iron cobaltites $\text{Co}_x\text{Fe}_{3-x}\text{O}_4$ ($1 \leq x \leq 2.46$) before and after spinodal decomposition, *J. Magn. Magn. Mater.* 334 (2013) 66–73.
- [49] J.Z. Msomi, T. Moyo, H.M.I. Abdallah, Magnetic properties of $\text{Mg}_x\text{Mn}_{1-x}\text{Fe}_2\text{O}_4$ nanoferrites, *J. Super. Cond. Novel Magnet* 25 (2012) 2643–2646.
- [50] R. Malik, S. Annapoorni, S. Lamba, V.R. Raghavendra, A. Gupta, P. Sharma, A. Inoue, Mössbauer and magnetic studies in nickel ferrite nanoparticles: Effect of size distribution, *J. Magn. Magn. Mater.* 322 (2010) 3742.